University of Florida
DE-SC0017715
Collaborative Research: The Role of
Grain Boundry Structure and Chemistry
in Materials Failure
8/1/2017-1/31/2022

Final Technical Report

K.E. Aifantis

The purpose of this project was to understand slip transmission across internal surfaces and relate it to the strength and chemistry of the internal surface. In doing so we followed an interdisciplinary approach that employed theory, experiments and molecular dynamic (MD) simulations. Our guideline was that interfaces are characterized by their own mechanically induced interface parameter. We began studying simple grain boundaries in Fe systems, and then moved on to graphene and nanolayer composites. A brief overview of some of our main results is given below.

1. Capturing slip transmission in BCC Fe with segregants through nanoindention

1.1. Experiments

Nanoindentaion Experiments on Fe-Si bicrystal

The first three years of the project were dedicated in verifying the ability of mechanically induced grain boundary terms to predict the mechanical response of GBs in Fe, with and without segregants, and for different GB geometries. As a first step nanoindentation experiments were used since it has been shown that indenting in close proximity to GBs allows for second pop-ins to be obtained in the load- displacement curve, which can be assumed to indicate slip transmission. A brief summary is provided below but detailed information can be found in our published paper [Journal of Materials Science 54, 1831-1843, 2019]. By indenting near GBs of Fe-3wt% Si and performing scanning probe microscopy it was possible to verify that indeed slip transmission was present when a secondary pop-in took place, as seen in Fig. 1.

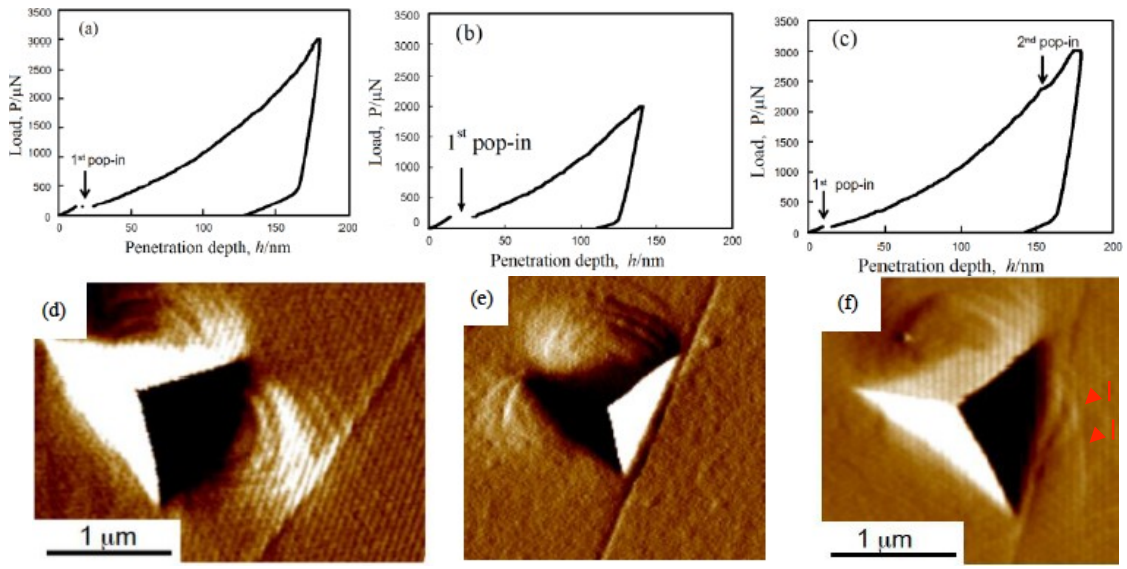

Fig. 1. Representative nanoindentation load-depth curves and SPM images obtained when the grain boundary had a 42.0°<100> misorientation: (a) indentation in the grain interior ; (b) indentation near the GB with the maximum load being 2 mN ; and (c) indentation near the GB with the maximum load being 3 mN ; (d) SPM image of indent in grain interior, taken after the curve shown in (a) ; (e) SPM image of surface after the indentation curve shown in (b) ; (f) SPM image of the surface after the indentation show in (c). It is seen that for the case that a second pop-in occurs slip is transmitted to the neighboring grain. Taken from [Journal of Materials Science 54, 1831-1843, 2019]. Arrows indicate slip transmission.

From the load-displacement curves it is possible to obtain an approximation through Tabor's rule of the stress present during the second pop-in, which corresponds to the GB yield stress, σ_{gb}, which is predicted by Eq. (2). Fitting the experimentally obtained points for σ_{gb} against the GB-indenter distance (d) to the analytical prediction from Eq. (3) showed that indeed ξ_{gb} was capable of capturing the resistance of GBs to deformation. Different grain boundary geometries were tested experimentally, as seen in Fig. 1(b), in order to explore the effect of the geometry on ξ_{gb}. Comparing the ξ_{gb} values obtained for the various GBs examined did not indicate a correlation with misorientation, however, a dependence on with the grain boundary plane was noted in, which is similar to the dependence of the thermodynamic grain boundary energy on misorientation and GB plane.

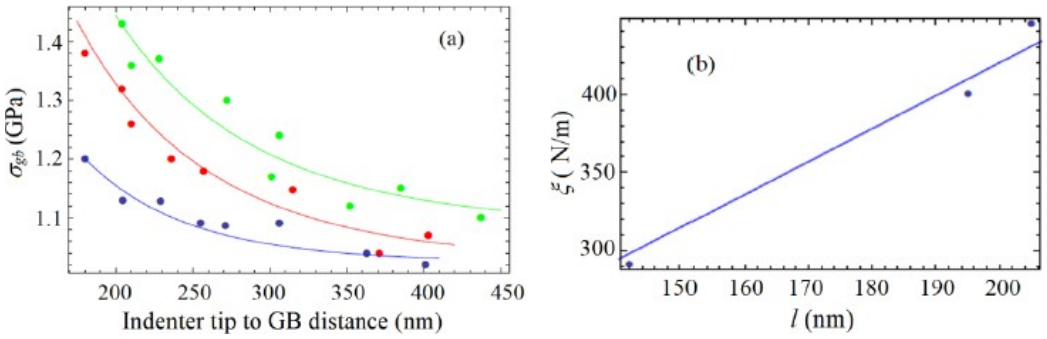

Fig. 2 (a) Fits of Eq. (3) to experimental data (dots) of the grain boundary yield stress in Fe-3wt%Si bicrystals. Each color indicates a different GB: green- 42°<110>,{120}A//{015}B, red- 22.5°<110>,{121}A//{211}B, blue- 44.6°<110>, {013}A //{323}B. (b) Plot of values obtained for ξ_{gb} and l; it is seen that a linear best fit is obtained. Taken from our published work [Journal of Materials Science 54, 1831-1843, 2019].

Relating interfacial gradient plasticity with the Hall-Petch equation, allowed to obtain the Hall-Petch slope in terms of the interface parameter : $k = 0.7 \cdot \xi(l)^{0.5}$. Using the values of ξ_{gb} and l obtained from the fits in Fig. 2, allowed to estimate k was as 0.12, 0.14 and 0.077 MPa m-1/2 for the 22.5°, 42.0°, and 44.6° GBs, respectively. Although the H-P slope for such Fe-3wt%Si systems has not been calculated by other means, the H-P slope for Fe-2.2wt% Si has been measured to be k~0.5 MPa $m^{-1/2}$ which is in the same order of magnitude as the prediction here. Indentation near GB, can therefore allow for the estimation of the H-P slope through the mechanical induced interface term ξ_{gb}, indicating a direct relationship between k and ξ_{gb} as was proposed in the first submission.

In order to further interpret the results of Fig. 2 dislocation mechanics considerations were used to define ξ_{gb} in terms of the shear modulus (G), the Burgers vector (b), the residual Burgers vector on the GB due to transmission (b_r), the grain boundary free volume (a_o) and the residual dislocation length (δ) according to the expression:

$$\xi_{gb} = 0.95 \cdot G \cdot \sqrt{3 \cdot b^2 + \frac{4 \cdot \delta \cdot b_r^2}{\pi^2 \cdot a_0}}.$$

The GB and dislocation quantities used to define ξ_{gb} can be obtained from MD compression studies on a bicrystals.

Compression of T91 steel annealed with molten LBE micropillars

In addition to the ability of our mechanically induced interfacial parameter to interpret indentation results

near grain boundaries, incorporating such interface terms can allow to capture the stress-strain curve obtained during the compression of T91 steel annealed with molten LBE micropillars. As seen in Fig. 3 (a) deformation in a batch of such pillars was governed by slip of high angle grain boundaries. The respective experimental and theoretical curves are shown in Fig. 3(b). As the theory and experimental are is such good agreement we experimentally obtained ξ_{gb} for various pillars, which was in the order of 2000N/m.

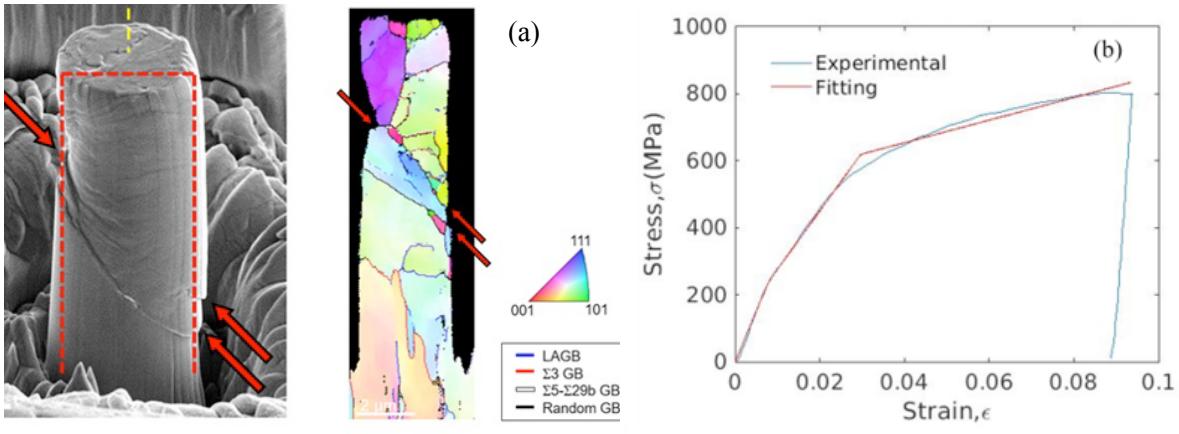

Fig. 3. (a) Scanning electron microscopy image of T91 steel annealed with molten LBE micropillar after compression [Kaede et al MRS Advances 3 (8-9) (2018) 419–425]. Pillar C appears to be sheared at an angle of about 45◦ to the tensile axis (as was indicated by the yellow dash line). IPF map of pillar deformed to a 9.4% nominal strain which showed the shear deformation along the high angle grain boundaries inclined at the angle of about 45◦ to the loading axis (as indicated by the arrow heads). (b) Comparisson between experimental stress-strain curve for pillar with interfacial gradient plasticity. Article under review.

1.2. Simulations

Although the results obtained for slip transmission through ex-situ indentation are promising, it is difficult to vary the segregation content. Therefore, MD indentation was initially carried out for pure Fe [Physica Status Solidi (b), 256, #1800370, 2019] or doped with either C or Si [article under review]. Similarly, as in the experiments distinct pop-ins occurred during dislocation formation. The occurrence of such pop-ins was more common, however, due to the sensitivity of the simulations to individual defect formation. The simulations allowed for a clear observation of the stress at which the GBs began deforming plastically. For most of the systems considered, thus far, significant dislocation absorption took place prior to transference and therefore σ_{gb} was computed at the onset plastic strain at the GB as seen in Fig. 4 (b). Comparing the simulation data with the analytical expression σ_{gb} for ($\sigma_{gb} = (\xi_{gb} / 2l)\coth(d / l)$) allowed to determine ξ_{gb} as 11.1N/m for pure Fe, 13.5N/m for Fe-0.3wt%Si and 11.9N/m for Fe-0.012wt%C, indicating that the segregation of C and Si increase ξ_{gb}. The results shown in Fig. 4 are for a Σ5 GB, however, additional configurations have been considered with different GB planes and also higher segregation contents in order to capture the interplay between segregation and GB structure.

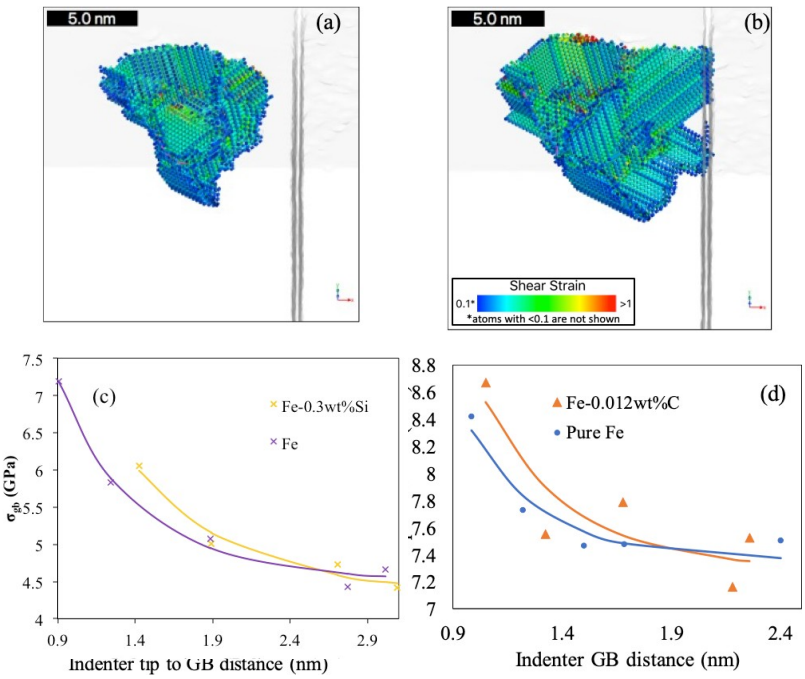

Fig. 4: (a)&(b) depict the strain field surrounding the indenter tip during indentation near a a Σ5 symmetric symmetric tilt GB in BCC Fe. In (a) the GB has not yielded, while in (b) GB yielding occurs as strain develops. From (b) it is possible to deduce the GB yield stress. In (c)&(d) the simulation data (points) are compared with the theoretical predictions (solid lines), allowing to determine the value for the interface parameter ξ_{gb}. C and Si segregant atoms are added to the GBs, allowing to determine how segregation affects ξ_{gb}. Results in publication under review.

It is interesting to note that with MD indentation it is possible to precisely indent directly on the GB allowing the calculation of the grain boundary yield stress, without contributions from the grain. These results have been published in [Kuhr, B.R., Aifantis, K.E., Interpreting the inverse Hall-Petch relationship and capturing segregation hardening by measuring the grain boundary yield stress through MD indentation Materials Science and Engineering: A, 745, 107-114, 2019] and allowed the interpretation of the inverse Hall-Petch expression that occurs in nanomaterials.

2. Capturing new dislocation-GB interaction mechanisms in BCC Fe with MD

In order to better understand the dislocation-grain boundary interactions we introduced a BCC bicrystal configuration for MD that allowed for dislocation pile ups, as seen in Fig. 5. Eight different GBs were considered for BCC Fe, and it was shown that the mechanisms by which slip transference occurred depended on the GB type [Acta Mater. 195, 358–370, 2020]. For all cases, the first few dislocations piled up at the GB; particularly each dislocation was fully absorbed upon the nucleation of the latter dislocation, which was in good agreement with recent *in-situ* TEM observations. Once the 4th or 5th dislocation approached the GB slip across the GB occurred, either by dislocation transmission, or twin formation (depending on the GB type). Previous MD studies, on the contrary, showed that dislocations would immediately transmit across the GB or reflect in single dislocation-GB interaction events. Of course, it should be noted that these studies are not for the same GB type or crystal structure, and therefore a true comparison among them cannot be done.

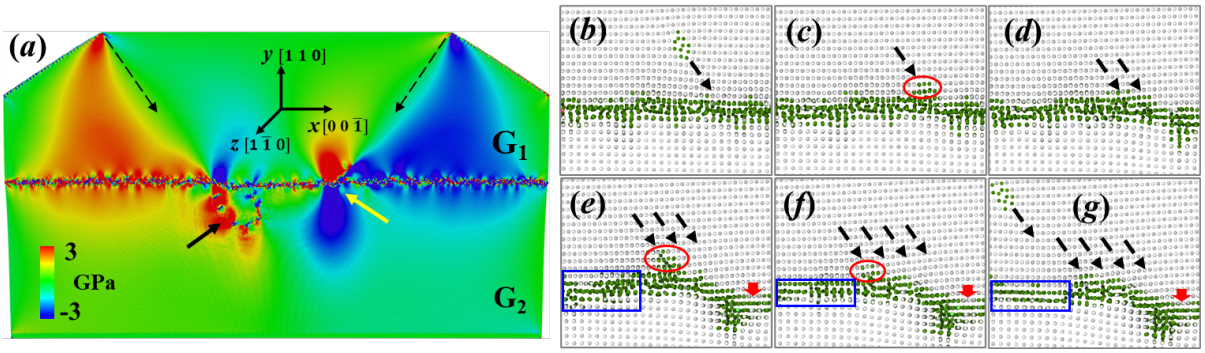

Fig. 5. (a) Dislocation-GB interactions for a twist 90.0˚ GB. The black arrow indicates the nucleated dislocation in grain 2 (G_2), the yellow arrow indicates the accumulated stress due to pileup, and the dashed arrows indicate the slip trace of edge dislocations. Atoms are colored by the atomic shear stress. (b-g) Defect atoms near a GB after different number of dislocations interacted with the GB. Defect atoms are identified by the Common Neighbor Analysis. Dashed arrow lines indicate the slip planes. Circles indicate the pileup. Rectangles indicate the atomic structure rearrangement due to dislocation-GB interactions. Red arrows indicate local GB migration. The image is taken from our published results [Acta Mater. 195, 358–370, 2020].

As seen in Fig. 5 as the GB interacted with each new incoming dislocation, the atomic structure at the GB was re-arranged and local GB migration occurred, indicating that the structural GB energy changes during deformation and the conventional thermodynamics energy is not sufficient for characterizing deforming GBs. An indirect experimental verification of these observations is that when dislocations were absorbed in a twin boundary (TB), they altered its structure and affected the subsequent dislocation-TB interactions. This suggests that the GB should be considered as an evolving interface with dynamic properties during deformation.

This setup allowed for the computation of the stress-strain (σ–ε) curve (Fig. 6(a)). The "second knee" which is seen to occur between state II and stage III was the stress at which the GB began deforming plasticity, and is termed GB yield stress (σ_{gb}). This dynamic GB behavior was understood through the mechanical interface energy $\varphi(\varepsilon^p)$ (as introduced within interfacial gradient plasticity [1]), which is a function of the plastic strain (ε^p) and the mechanical interface parameter ξ_{gb}. This theory predicts that $\sigma_{gb} = \sigma_0 + \xi_{gb}/(2l)\coth\left(D/l\right)$, where σ_0 is the yield stress (first "knee" in Fig. 6(a)), D is the grain size and l is the internal length. Therefore, ξ_{gb}, was obtained by fits to the simulation data. The dependence of ξ_{gb} on the residual Burgers vector and internal length were examined (Fig. 6(b)), indicating that for a particular GB type, the values of ξ_{gb} are positively related to the magnitude of the residual Burgers vector. Since the residual Burgers vector is related to the mechanical strength of a GB, the proposed interface parameter ξ_{gb} can be used as an effective and measurable parameter to quantify the strength of a GB.

The segregation effect on the GB strength was studied by introducing different H at% content at the GB (H was chosen as the Fe-H potential was more stable than the others considered). The observed increase of ξ_{gb} on H content in Fig. 6(c) can be explained from the GB-mediated dislocation absorption. As the H content increased, it was shown that the rearrangement region in the GB got wider and both Fe and H atoms were rearranged to accommodate the deformation due to absorption, leading to a higher ξ_{gb}. This was consistent with the earlier mentioned MD studies, which showed GB strengthening with the addition of H in metals.

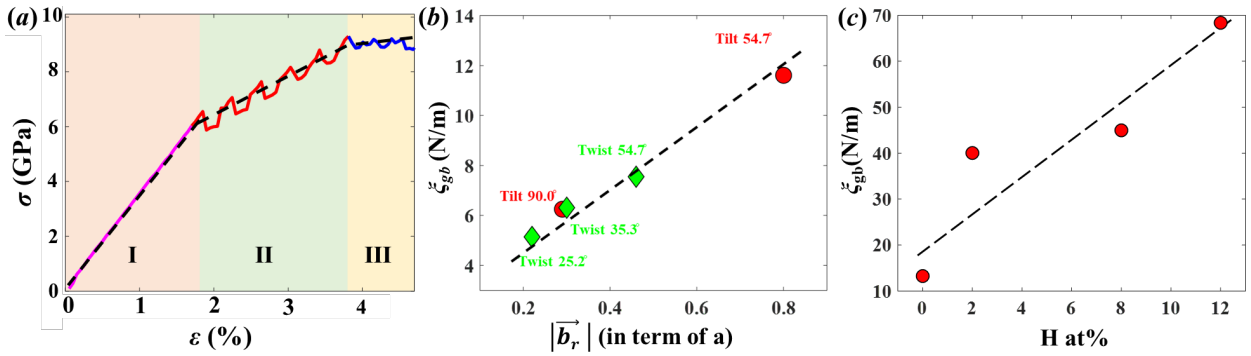

Fig. 6 (a) Stress-strain curve of twist 90˚ GB (solid line) and fit from interface gradient plasticity (dashed line), stage I denote elasticity, stage II plasticity in the upper grain, and stage III GB yielding and slip transmission; (b) Plot of the mechanical interface energy parameter ξ_{gb} versus the magnitude of the residual Burgers vector; (c) Variation of ξ_{gb} with respect to different H contents for the 54.7˚ tilt GB bicrystal. Results are taken from our published paper [Acta Mater. 195, 358–370, 2020].

3. Capturing dislocation-graphene interaction mechanisms in metal composites

In an attempt to create an infinitely stiff interface, we inserted graphene nanosheets in a BCC Fe single crystal [Applied Surface Science 535, 147602, 2021], using a configuration similar to that of Fig. 5. Compression with a flat indenter tip allowed the nucleation of dislocations from the top edges (Fig. 7(*a*)). The first dislocation was absorbed by the Fe/graphene interface (Fig. 7(*b*)), the second dislocation was blocked by the graphene (Fig. 7(*c*)), and the third dislocation transmitted across the graphene directly (Fig. 7(*d*)). This was an unexpected atomic observation indicating that dislocations can transfer across graphene without fracture of the graphene. Therefore, even though graphene did not behave as an infinitely stiff interface, and is not a GB which is the focus of our hypothesis, this work does illustrate the possible transition mechanisms in the interaction between consecutive dislocations and GBs. The graphene strength was quantified through the mechanical interface parameter $\xi_{graphene}$, by relating the (σ–ε) curves of the simulation with interfacial gradient plasticity. $\xi_{graphene}$ was obtained as 11.49 N/m for monolayer graphene and increased as the graphene layers increased (since slip was transmission became more difficult) or by introducing an amorphous metal layer between the graphene and Fe, which again impeded transmission. This indicates that ξ_{gb} can be a unified measure for understanding the strength of a GB as its atomic structure and GB free volume is modified, which be done with impurity atoms.

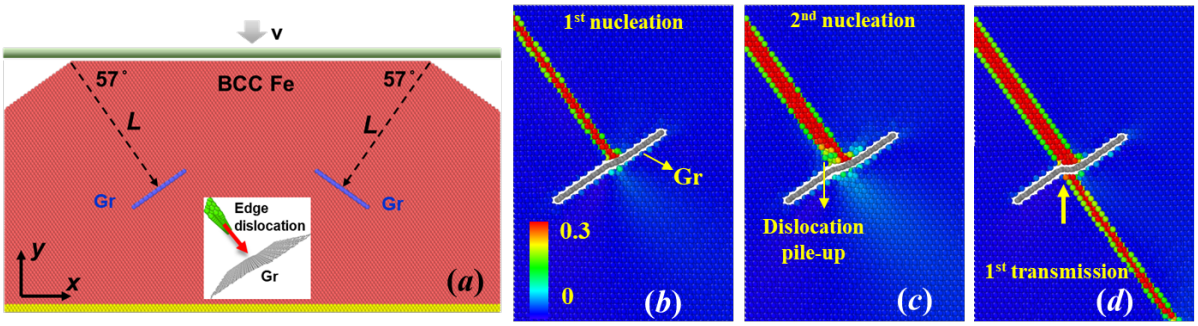

Fig. 7 (*a*) Compression simulation setup for studying the interaction of dislocations with graphene; (*b-d*) atomic shear strain of Fe atoms at different stages of dislocation-graphene interactions. Image taken from our paper [Applied Surface Science 535, 147602, 2021].

Dislocation-Graphene interactions in Cu-Graphene composites were also studied systematically in our recent manuscript [Carbon 172, 50-70, 2021] using two carefully selected configurations: (i) edge dislocations in pileups interacting with graphene during nanoindentation and (ii) complex dislocations interacting with graphene during the compression of layered nanopillars. The intrinsic and extrinsic size effects were investigated with respect to varying the Cu lamella thickness and pillar sizes, revealing an anomalous extrinsic size effect: the smaller, the weaker. It was also revealed that edge dislocations in the pileup could easily transmit across the graphene through sliding at the Cu/graphene interface and graphene reorientation, whereas the transmission of complex dislocations was much more difficult.

4. Strengthening transitions in crystalline-amorphous nanolaminates through molecular dynamics

Interchanging crystalline-amorphous nanolaminates are another system, which is rather new and its deformation mechanisms as a function of its alternating layer structure has not been examined are. A unique nanoindentation configuration was set up that allows for the continuous emission of a pair of edge dislocations in the same slip planes as dislocation sources, revealing the different interaction mechanisms between dislocations and amorphous layers of varying thickness. This allows to study the transmission of plastic strain from the crystalline to amorphous, and amorphous to crystalline layers. It is found that the thickness of the amorphous layer controls the deformation mechanism, as it is seen that a thin amorphous layer acts as an obstacle to dislocation motion, while a thick one acts as a dislocation sink. As a result, shear transformation zones and mature shear bands form in the amorphous layer as its thickness increases. These findings can be used to guide the design of crystalline-amorphous nanolaminates. A representative image when the amorphous thickness is small is shown in Fig. 8.

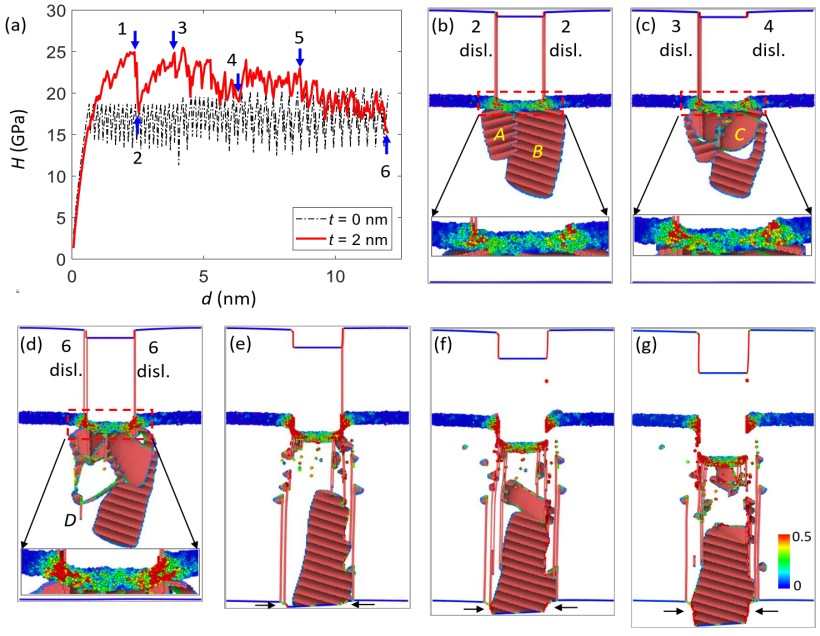

Fig. 8: Simulation results of a crystalline amorphous nanolaminate when the amorphous thickness is t = 2 nm. (a) Hardness-depth (H-d) curves. (b-g) Generated plasticity due to indentation in the system at points 1-6 in (a). Dislocations and stacking faults are identified by common neighbor analysis in crystalline layers. Atoms in the amorphous layer are colored by atomic shear strain with the colormap in (g).

5. Conclusions

It can be seen from the above overview that throughout the project we were able to validate our hypothesis that the mechanical behavior of materials which contain internal surfaces is controlled by a mechanically induced interface parameter. New dislocation-grain boundary interaction mechanisms were revealed and the strengthening effects of non-traditional interfaces such as graphene and an crystalline-amorphous layer nanolaminates were illustrated. Our work can therefore aid in designing materials with tunable mechanical behavior based on their interfacial type.

Published articles

1. Soman, P.P., Herbert, E.G., Aifantis, K.E., Hackney, S.A., Effect of Processing on Nix-Gao Bilinear Indentation Results Obtained for High Purity Iron, MRS Advances 3, 477-486, 2018.

2. Aifantis K.E., Deng H., Shibata H., Tsurekawa S., Lejček P., Hackney S.A., Interpreting slip transmission through mechanically induced interface energies: a Fe–3%Si case study, Journal of Materials Science 54, 1831-18431, 2019. 10.1007/s10853-018-2929-5

3. Kuhr B.R., Aifantis, K.E., The Formation and Evolution of Defects in Nanocrystalline Fe During Indentation: The Role of Twins in Pop-Ins, Physica Status Solidi (b), 256, article # 1800370 (6 pg), 2019. 10.1002/pssb.201800370

4. Prasad P.SG, Herbert E.G., Aifantis K.E., Hackney S.A., Analysis of local grain boundary strengthening utilizing the extrinsic indentation size effect. J. Materials Science 34, 2347- 2369, 2019. https://doi.org/10.1557/jmr.2019.102

5. Kuhr B.R.P, Aifantis, K.E., Interpreting the inverse Hall-Petch relationship and capturing segregation hardening by measuring the grain boundary yield stress through MD indentation, Materials Science and Engineering: A 745, 107-114, 2019. https://doi.org/10.1016/j.msea.2018.12.053

6. Shuang F.G, Aifantis, K.E, Modelling Dislocation-Graphene Interactions in a BCC Fe Matrix by Molecular Dynamics Simulations and Gradient Plasticity Theory, Applied Surface Science 535, 147602, 2021. https://doi.org/10.1016/j.apsusc.2020.147602

7. Shuang F.G, Aifantis, K.E, Using molecular dynamics to determine mechanical grain boundary energies and capture their dependence on residual Burgers vector, segregation and grain size, Acta Materialia 195, 2020, 358-370, 2020. https://doi.org/10.1016/j.actamat.2020.05.014

8. Shuang F.G, Aifantis, K.E., Relating the strength of graphene/metal composites to the graphene orientation and position, Scripta Materialia 181, 70-75, 2020. https://doi.org/10.1016/j.scriptamat.2020.02.014

9. Shuang F.G, Dai Z., Aifantis K.E., Strengthening in Metal/Graphene Composites: Capturing the Transition from Interface to Precipitate Hardening, ACS Applied Materials and Interfaces 13, 26610 – 266209, 2021. https://doi.org/10.1021/acsami.1c05129

10. Shuang F.G, Aifantis, K.E, Dislocation-graphene interactions in Cu/graphene composites and the effect of boundary conditions: a molecular dynamics study, Carbon 172, 50-70, 2021. https://doi.org/10.1016/j.carbon.2020.09.043

11. Parisis K., Shuang F., Wang B., Hu P., Giannakoudakis A., Konstantinidis A., From Gradient Elasticity to Gradient Interatomic Potentials: The Case-Study of Gradient London Potential, Journal of Applied Mathematics and Physics 08(09):1826-1837, 2020. http://dx.doi.org/10.4236/jamp.2020.89137

12. Shuang F, Wang B., Aifantis K.E., Revealing multiple strengthening transitions in crystalline-amorphous nanolaminates through molecular dynamics. Under Review

13. Wang B., Kaede K, Tsurekawa S., Aifantis K.E., Capturing the Softening in T91 Steel Annealed with Molten LBE through Mechanical Interface Energy Terms, Under Review

14. Shuang F., Kuhr B., Aifantis K.E., Capturing the effect of grain boundary segregation on slip transmission during indentation, Under Review

Noted Invited Talks

1. K.E. Aifantis, Slip Transmission in Ultra Fine Grain Materials, Invited Talk, TMS 2020, San Diego, CA.

2. K.E. Aifantis, F. Shuang, Mechanical Interface Energies that Capture Dislocation Transmission, Invited Talk, 2019 MRS, Phoenix, AZ.

3. Using atomistic simulations to illustrate how grain boundary chemistry governs defect formation in nanocrystalline Fe, Invited Talk, European Materials Research Society Spring Meeting 2018, Strasburg, France, 2018.

4. Interfaces in Nanomaterials, Keynote Talk, Sustainable Industrial Processing Summit & Exhibition 2017, Cancun, Mexico 2017.

5. Mechanically induced interface energy terms, Invited Talk, 14th International Conference on Fracture, Rhodes, Greece, 2017.